ADVANCES IN Sampling Theory and Techniques

Leonid P. Yaroslavsky

SPIE PRESS
Bellingham, Washington USA

Library of Congress Cataloging-in-Publication Data

Names: Yaroslavsky, L. P. (Leonid Pinkhusovich), author.
Title: Advances in sampling theory and techniques / L. Yaroslavsky.
Description: Bellingham, Washington : SPIE, [2020] | Includes bibliographical references and index.
Identifiers: LCCN 2019042348 | ISBN 9781510633834 (paperback) | ISBN 9781510633841 (pdf) | ISBN 9781510633858 (epub) | ISBN 9781510633865 (kindle edition)
Subjects: LCSH: Signal processing–Digital techniques–Mathematics. | Image processing–Digital techniques–Mathematics. | Fourier transformations.
Classification: LCC TK5102.9 .I225 2020 | DDC 621.382/20151952–dc23
LC record available at https://lccn.loc.gov/2019042348

Published by

SPIE
P.O. Box 10
Bellingham, Washington 98227-0010 USA
Phone: +1 360.676.3290
Fax: +1 360.647.1445
Email: books@spie.org
Web: http://spie.org

Printed in the United States of America.
Last updated 5 March 2020
For updates to this book, visit http://spie.org and type “PM315” in the search field.
Cover image courtesy of udi Steinwell.

SPIE.

Contents

Preface

Signal sampling is the major method for converting analog signals into sets of numbers that form digital models of the signals. The key issues in the sampling theory and practice are

- What is the minimal amount of numbers, or what is the minimal sampling rate, sufficient to represent analog signals with a given accuracy?
- What kinds of signal distortions are caused by their sampling?
- What signal attributes determine the minimal sampling rate?
- How can one sample signals with sampling rates close to the theoretical minimum?
- Is it possible to resample sampled signals without introducing additional distortions due to the resampling?
- What are adequate discrete representations of signal transforms, such as convolution and Fourier transforms?

All of these issues are addresed in this book, supplemented by MATLAB® exercises, which you can download via the following link: http:/spie.org/Samples/Pressbook_Supplemental/PM315_sup.zip

Researchers, engineers, and students will benefit from the most updated formulations of the sampling theory, as well as practical algorithms of signal and image sampling with sampling rates close to the theoretical minimum and interpolation-error-free methods of signal/image resampling, geometrical transformations, differentiation, and integration.

Leonid Yaroslavsky
December 2019

Chapter 1
Introduction

1.1 A Historical Perspective of Sampling: From Ancient Mosaics to Computational Imaging

It is easier to grasp a subject by tracing its evolution. Sampling as a mechanism for image formation was first developed by nature in the form of compound and retinal eyes (Figs. 1.1 and 1.2).

Light-sensitive cells (photoreceptors) of the eyes convert the luminosity of small individual areas around different points of observed objects into signals that are sent to the visual cortex of the brain, thus creating an object image.

At the dawn of human culture, ancient people discovered that small pieces of glass, pottery, or small tiles placed together in an appropriate order create a picture (Fig. 1.3). This led to the art of mosaic, which appeared throughout the world. In Byzantium, from the 4th to 14th centuries, it became the leading form of pictorial art.

Ancient artists knew how to intuitively choose the size of the tiles to make good-quality mosaic pictures with the minimal number of tiles. They taught their apprentices that skill; however, no "sampling theory" governed their knowledge, and no need for such a theory existed.

Such a need arose with the creation of the first electrical communication devices. Shortly after the early commercial success of telegraphy in the 1840s, engineers attempted to send more than one signal over a single wire and over increasingly larger distances. In 1854, the first transatlantic telegraph cable project began.[1] The first official telegram to pass between two continents was a letter of congratulations from Queen Victoria of the United Kingdom to the President of the United States, James Buchanan, on August 16, 1858.

However, the signal quality declined rapidly, slowing transmission to an almost unusable speed. The Atlantic Telegraph Company's chief electrician, E. O. W. Whitehouse, decided that the reason for the low speed of transmission was insufficiently high voltage, and so he applied excessive voltage to the cable in the hope of achieving faster operation. The excessive voltage destroyed the cable.[1]

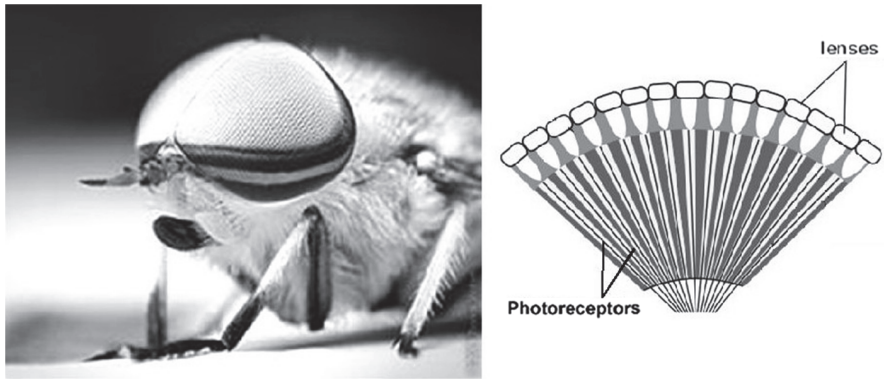

Figure 1.1 Anatomy and structure of compound eyes of insects.

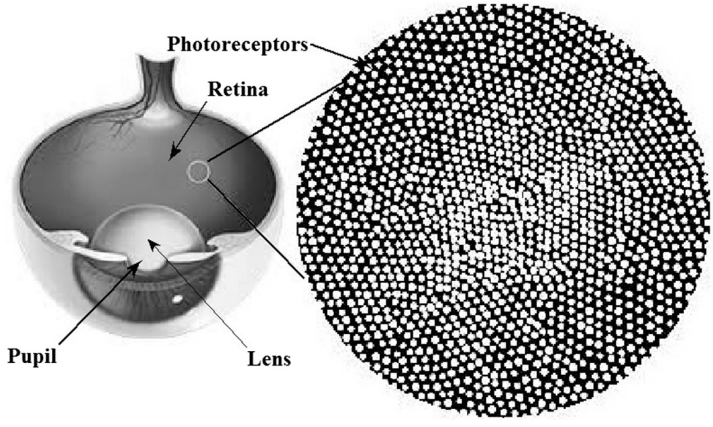

Figure 1.2 The retinal eye of vertebrates.

To explain and solve the problem, the company invited famous physicist Sir William Thomson, who sought to apply his theory of heat propagation. In particular, he used Fourier series to solve differential equations.

After accumulating sufficient experience in the transmission of telegraph and, later, sound and image signals, communication engineers eventually understood that the speed of information transmission is limited by the wave bandwidth of communication channels. This is what one of the founders of communication theory, Dennis Gabor, wrote in his seminal paper[2] in 1944:

> The principle that the transmission of a certain amount of information per unit time requires a certain minimum wave-band width dawned gradually upon communication engineers during the third decade of this (20-th) century. Similarly, as the principle of conservation of energy emerged from slowly hardening conviction of impossibility of perpetuum mobile, this fundamental principle of communication

considerable popularity and initiated a steady flow of publications demonstrating its applicability in different applications.

Although it eventually turned out that the compressed sensing methods still require certain redundancy in signal sampling, the concept of signal sparsity as a generalization of the classic concept of signal-band limitations proved to be very fruitful. It stimulated reformulation of the sampling theory in terms of signal sparsity, the proof that signal sparsity defines the minimal signal sampling rate sufficient for signal reconstruction with the accuracy that corresponds to the level of its sparsity, and the demonstration that this minimal sampling rate can be achieved using the means of computational imaging.[12,13]

1.2 Book Overview

The book is divided into two parts, supplemented with MATLAB-based exercises. The first part (Chapters 2 to 7) is devoted to different aspects of signal sampling.

Chapter 2 begins with the classic formulation (Section 2.1) of the sampling theorem for 1D band-limited signals. It is then extended in Section 2.2 to sampling 1D band-limited band-pass signals and, in Section 2.3, to band-limited 2D signals, for which the concept of optimal 2D regular lattices is introduced. Section 2.4 deals with sampling distortions, which take place when sampling real, non-band-limited signals. In Section 2.5, a realistic reformulation of the sampling theorem is provided that does not assume the band-limitedness of signals and is based on mathematical models of real signal sampling and reconstruction devices, as well as the realization that no precise signal reconstruction from a sampled representation is possible. The last two sections of the chapter address, through two complementary approaches, the problem of evaluating the minimal sampling rate sufficient for signal reconstruction with a given accuracy. In Section 2.6, sampling of signal subband decompositions is considered as a model of sampling with the minimal sampling rate, and in Section 2.7, a formulation of the discrete sampling theorem and its extension to continuous signals are provided for use in Chapters 3 and 4.

Chapter 3 is devoted to demystifying the concept of compressed sensing. First, in Section 3.1, the ubiquitous compressibility of images sampled using the standard regular sampling methods is demonstrated and explained with examples of sampled images. In Section 3.2, the concept of compressed sensing is elucidated with a simple model that demonstrates how and under what conditions can one precisely reconstruct a signal sampled with aliasing, i.e., sampled by violating the sampling theorem. In Section 3.3, the sampling redundancy required by compressed sensing methods for precise signal reconstruction is estimated to evaluate how far these methods are from reaching the minimal signal sampling rates.

Chapter 2
Sampling Theorems

2.1 Kotelnikov–Shannon Sampling Theorem: Sampling Band-Limited 1D Signals

Kotelnikov's and Shannon's classic formulation of the sampling theorem reads as follows.[7,8]

Theorem: If a function of time $a(t)$ contains no frequencies higher than $F/2$ cycles per second (cps), it is completely determined by giving its ordinates at a series of points spaced $1/F$ seconds apart:

$$a(t) = \sum_{k=-\infty}^{\infty} a(k/F) \frac{\sin[\pi F(t - k/F)]}{\pi F(t - k/F)}. \tag{2.1}$$

The proof of this theorem is based on the properties of the integral Fourier transform (Appendix A1). Let $\alpha(f)$ be the Fourier spectrum of $a(t)$:

$$\alpha(f) = \int_{-\infty}^{\infty} a(t) \exp(i2\pi f t) dt \tag{2.2}$$

and

$$\alpha(|f| > F/2) = 0,$$

i.e.,

$$a(t) = \int_{-\infty}^{\infty} \alpha(f) \exp(-i2\pi f t) df = \int_{-F/2}^{F/2} \alpha(f) \exp(-i2\pi f t) df. \tag{2.3}$$

In the interval $[-F/2, F/2]$, the function $\alpha(f)$ can be represented by its Fourier series

$$\alpha(f) = \mathrm{rect}\left(\frac{f}{F}\right) \sum_{k=-\infty}^{\infty} \alpha_k \exp\left(i \frac{2\pi k f}{F}\right), \tag{2.4}$$

where

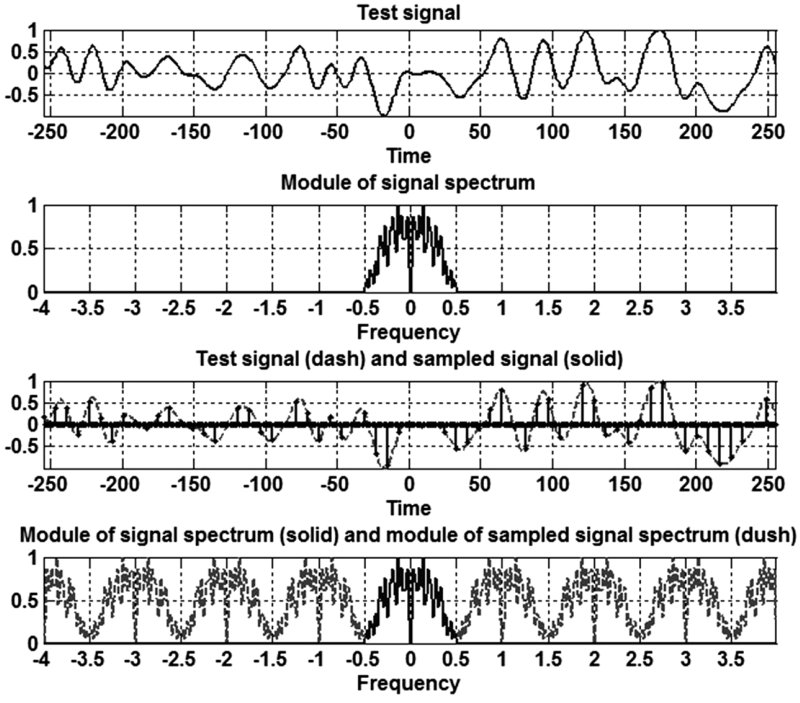

Figure 2.1 Interpretation of signal sampling to generate a virtual discrete signal with a Fourier spectrum formed by the periodically replicated Fourier spectrum of the signal. From top to bottom: a test signal, its Fourier spectrum, a virtual discrete signal comprising samples of the test signal, and its Fourier spectrum.

The sampling theorem implies that the number of samples of band-limited signals with bandwidth $[-F/2, F/2]$ per unit of signal length, i.e., the signal sampling rate, equals F. This rate is called the *Nyquist sampling rate*, a name that was coined by Shannon[8] in recognition of Nyquist's important contributions to communication theory.

The Nyquist sampling rate F is the minimal sampling rate sufficient to reconstruct band-limited signals from their samples. If the signal sampling rate is lower than F, the period of the periodic spectrum replication due to signal sampling will be lower than the spectrum width. Therefore, the signal spectrum will overlap with its periodic replicas and cannot be separated by the ideal low-pass filter without distortions.

2.2 Sampling 1D Band-Pass Signals

1D band-limited signals treated in the previous section are called *baseband signals*. Their Fourier spectrum is concentrated within a bounded interval $[-F/2, F/2]$ around zero frequency. This interval is called the *signal baseband*.

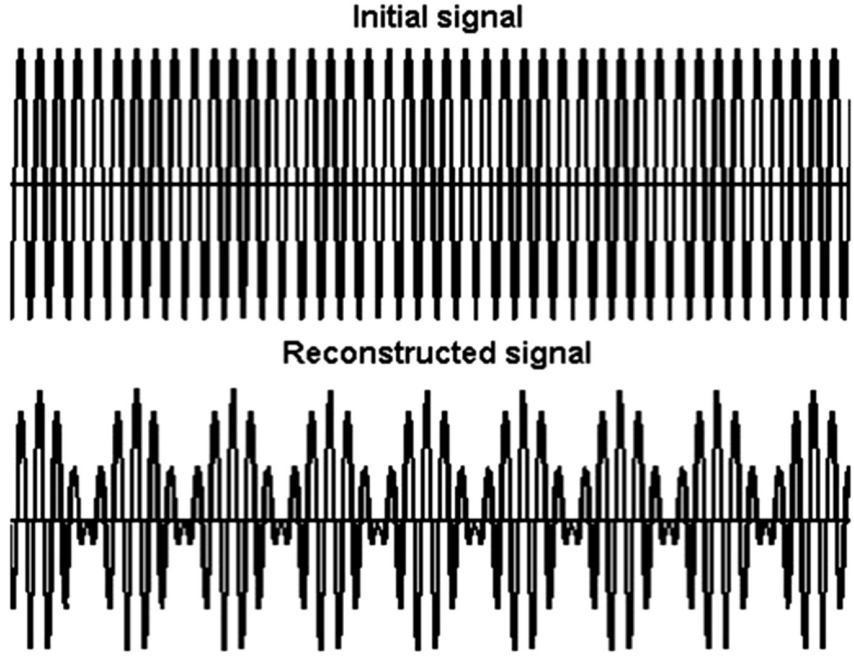

(a)

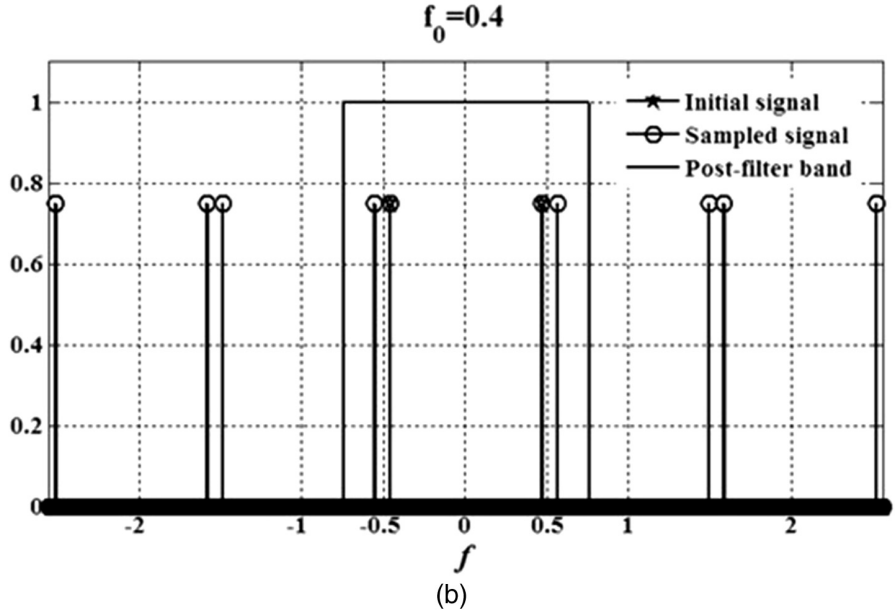

(b)

Figure 2.7 Moiré effect in sampling and reconstruction of a sinusoidal signal: (a) test signal of frequency $f_0 = 0.4$ (fraction of the sampling baseband width) and this signal sampled and reconstructed; (b) spectra of the test and sampled test signals for the case where the bandwidth of the reconstruction filter [−0.6, 0.6] exceeds the baseband [−0.5, 0.5] defined by the signal sampling rate.

2.7 The Discrete Sampling Theorem and Its Generalization to Continuous Signals

2.7.1 Theorem formulation

This section supports the above formulated statement of the sampling theorem that the minimal sampling rate of signals per unit of its size sufficient for signal reconstruction with a given MSE σ^2 equals the size S_{Secz} of the signal spectral EC zone that contains a $(E-\sigma^2)/E$ fraction of the signal energy by an alternative approach based on the the discrete sampling theorem and its generalization to continuous signals. This approach assumes direct signal sampling and opens a way to practical algorithms that allow one to reach the minimal rate.

Consider the following discrete model. Let $\mathbf{A}_N$ be a vector of N samples $\{a_k\}_{k=0,...,N-1}$ of a discrete signal, Φ_N be an $N \times N$ orthonormal transform matrix, composed of orthonormal basis functions $\{\varphi_r(k)\}$

$$\Phi_N = \{\varphi_r(k)\}_{r=0,1,...,N-1}, \tag{2.43}$$

and Γ_N be a vector of signal transform coefficients $\{\gamma_r\}_{r=0,...,N-1}$ such that

$$\mathbf{A}_N = \Phi_N \Gamma_N = \left\{ \sum_{r=0}^{N-1} \gamma_r \varphi_r(k) \right\}_{k=0,1,...N-1}. \tag{2.44}$$

Assume that only $K < N$ signal samples $\{a_{\tilde{k}}\}_{\tilde{k} \in \tilde{\mathbf{K}}}$ are available, where $\tilde{\mathbf{K}}$ is a K-size subset $\{\tilde{k}\}$ of indices $\{0,1, .., N-1\}$. These available K signal samples define a system of K equations:

$$\left\{ a_{\tilde{k}} = \sum_{r=0}^{N-1} \gamma_r \varphi_r(\tilde{k}) \right\}_{\tilde{k} \in \tilde{\mathbf{K}}} \tag{2.45}$$

for K signal transform coefficients $\{\gamma_r\}$ of certain K indices r.

Select a subset $\tilde{\mathbf{R}}$ of K transform coefficients indices $\{\tilde{r} \in \tilde{\mathbf{R}}\}$ and define a "KofN"-bounded spectrum approximation $\hat{A}_N^{(BS)}$ to the signal $\mathbf{A}_N$ as

$$\hat{\mathbf{A}}_N^{(BS)} = \left\{ \hat{a}_k = \sum_{\tilde{r} \in \tilde{R}} \gamma_{\tilde{r}} \varphi_{\tilde{r}}(k) \right\}. \tag{2.46}$$

Rewrite this equation in a more general form that involves all transform coefficients:

$$\hat{\mathbf{A}}_N^{BS} = \left\{ \hat{a}_k = \sum_{r=0}^{N-1} \tilde{\gamma}_r \varphi_r(k) \right\}, \tag{2.47}$$

Chapter 3
Compressed Sensing Demystified

3.1 Redundancy of Regular Image Sampling and Image Spectra Sparsity

As mentioned previously, contemporary digital display devices and image processing software imply by default that sampling over regular square sampling lattices is used for image sampling. For such a sampling, the image sampling interval $(\Delta_x, \Delta_y = \Delta_{xy})$ is supposed to be chosen so that the square sampling baseband $[-1/2\Delta_{xy} \le f_x \le 1/2\Delta_{xy}, -1/2\Delta_{xy} \le f_y \le 1/2\Delta_{xy}]$ in the image Fourier domain (f_x, f_y) fully embraces the image spectrum EC zone for the given accuracy of image reconsruction. This means that the area $1/\Delta_{xy}^2$ of this square zone, by necessity, exceeds the area of image spectrum EC zone, which, by virtue of the general sampling theorem, defines the minimal sampling rate sufficient for image reconstruction with the required MSE. Threrefore, conventional regular image sampling is generally redundant. It would be instructive to numerically evaluate this sampling redundancy of sampled natural images.

Figure 3.1 presents a set of ten test images along with estimations of their Fourier-spectrum EC zones. The Fourier spectra of the images were estimated using the DFT as a discrete representation of the integral Fourier transform (see Appendix A2). In order to avoid spectrum estimation errors due to boundary effects as much as possible, images were multiplied before spectral analysis by a circular apodization mask to smoothly bring them down to zero at the edges of the sampled region. Highlighted in the figures of image spectra are spectral EC zones that contain the largest image spectral components sufficient for image reconstruction with the same MSE as that of the image JPEG compression implemented by MATLAB.

These figures show that the spectral EC zones of all images occupy only a fraction of the area of the sampling baseband. This fraction, i.e., the ratio of the area of the image spectrum EC zone to the area of the sampling baseband,

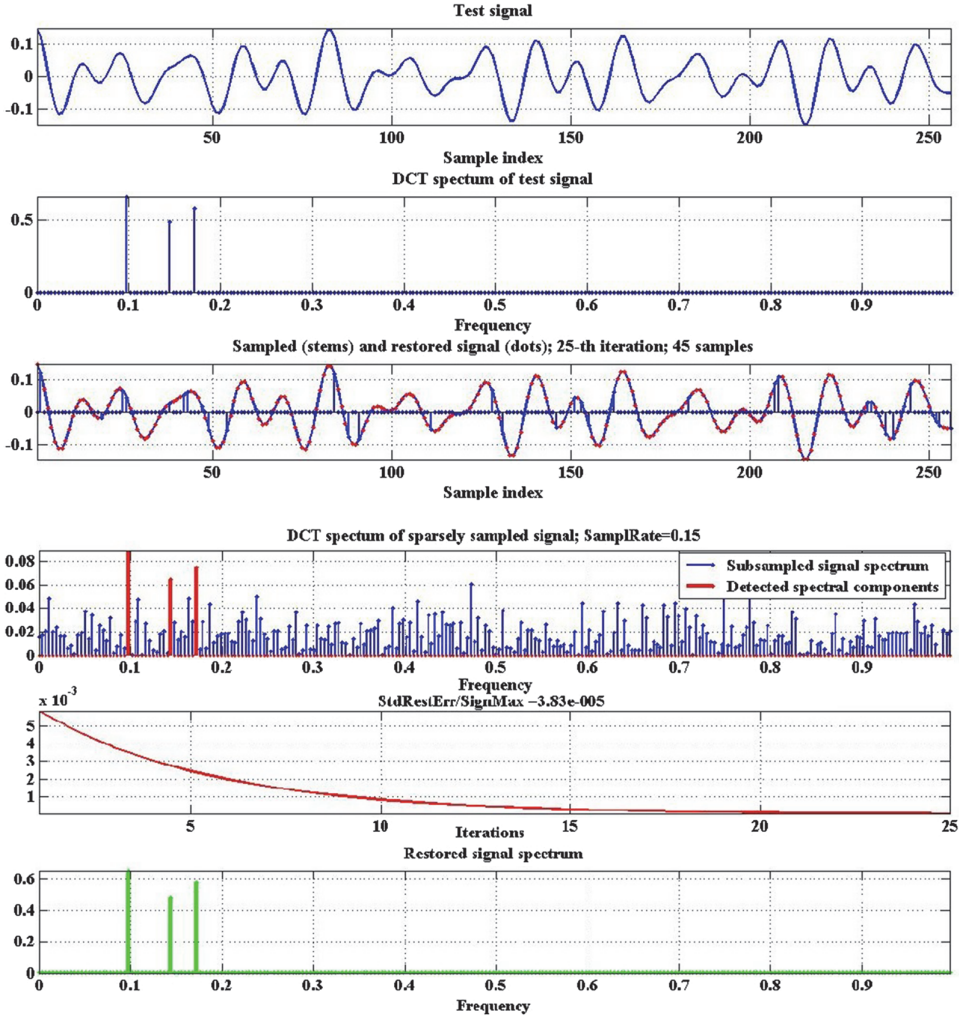

Figure 3.2 From top to bottom: test signal composed of three sinusoidal components; its DCT spectrum; this signal randomly sub-sampled (stems) and reconstructed (solid line); DCT spectrum of the sub-sampled signal; plot of the reconstruction RMSE vs. the number of reconstruction iterations; and the DCT spectrum of the reconstructed signal. The frequency is given in fractions of the width of the sampling baseband.

of the reconstructed signal DCT spectrum (the sixth plot) show that virtually precise reconstruction of the signal is achieved after a couple of tens of iterations: after 25 iterations, the reconstruction RMSE is 3.8×10^{-5}. Note that in this example the signal spectrum sparsity is $Ss = 3/256 \approx 1.2 \times 10^{-2}$, and therefore the sampling redundancy (ratio of the sampling rate to signal spectrum sparsity) is $R = M/K = 38/3 \cong 12.7$.

When the signal sub-sampling rate is too low and aliasing is severe, reliable detection of the signal spectral components in the spectrum of the

Chapter 4
Image Sampling and Reconstruction with Sampling Rates Close to the Theoretical Minimum

4.1 The ASBSR Method of Image Sampling and Reconstruction

This chapter describes a method of image sampling and reconstruction with sampling rates close to the minimal rate defined by the sampling theory. We begin with a formulation of a discrete model, for which the discrete sampling theorem holds.

The theorem implies the following image sampling and reconstruction protocol:

- Choose the number N of image samples required for image display and processing.
- Choose an image sparsifying transform.
- Specify a desired spectrum energy compaction zone of the image spectrum, i.e., a set of $M \leq N$ transform coefficients to be used for image reconstruction.
- Measure M image samples.
- Use M image samples to determine M transform coefficients of the chosen EC zone.
- Set the $N - M$ transform coefficients to zero and use the obtained spectrum to reconstruct the required N image samples by applying the inverse transform to the formed signal spectrum.

Consider possible ways to implement this principle:

Choosing a transform. The choice of transform is governed by the transform's energy compaction capability, i.e., the ability to compact most of the image signal energy into a small number of transform coefficients. An additional requirement is the availability of a fast transform algorithm. From

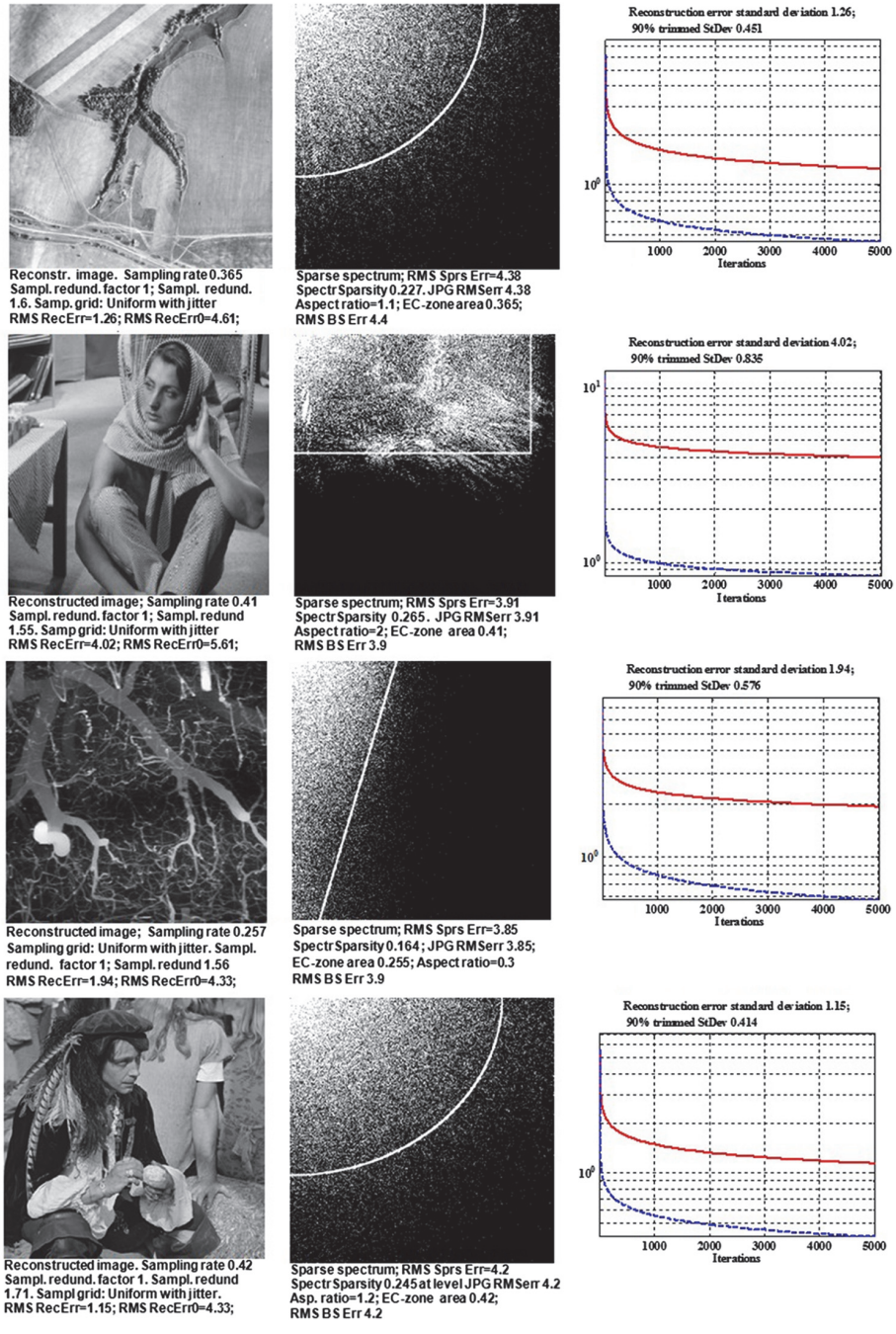

Figure 4.5 Results of experiments on the sampling and reconstruction of test images. From top to bottom: "AerialPhoto512," "Barbara512," "BloodVessels512," and "Pirate1024." From left to right: reconstructed images; EC zones of image spectra (white dots) and borders of the corresponding chosen-spectrum EC zone approximating shapes (white solid line); plots of the RMSE of all (solid line) and of the smallest 90% (dashed line) reconstruction errors vs. the number of iterations.

Chapter 5
Signal and Image Resampling, and Building Their Continuous Models

5.1 Signal/Image Resampling as an Interpolation Problem; Convolutional Interpolators

Many image processing applications must resample available digital images in positions other than the original ones. Such applications include fusing image data from different image modalities, building image mosaics from many partly overlapped images, reconstructing images from projections, producing image super-resolution from video sequences, stabilizing video images distorted by atmosphere turbulence, locating targets, and tracking with sub-pixel accuracy, to name a few.

Image resampling assumes that approximations of the original non-sampled images are built by interpolating available image samples and then resampling the obtained models in the required new positions. The most feasible and amenable to optimization is signal interpolation by means of digital convolution:

$$\tilde{a}_k = \sum_{n=0}^{N-1} h_n^{(\text{intp})} a_{k-n}, \tag{5.1}$$

where $\{\tilde{a}_k\}$ are samples of a signal obtained as a result of resampling the initial signal samples $\{a_k\}$, $\left\{h_n^{(intp)}\right\}$ are samples of the interpolation filter point spread function (PSF), and N is the number of available signal samples.

The problem of interpolating numerical data is one of the classic mathematical problems that can be traced back to Babylonian times.[22] Mathematical geniuses such as Newton, Euler, and Gauss contributed to its solution. Presently, numerous interpolation methods are known. The most popular in signal and image processing are convolutional methods, from the

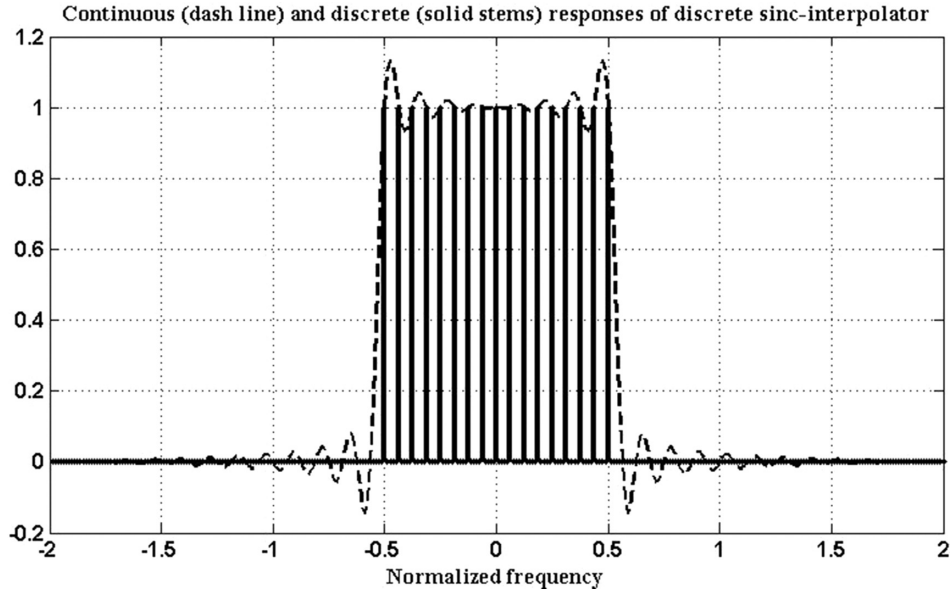

Figure 5.2 Continuous (solid line) and discrete (solid stems) frequency responses of the discrete sinc interpolator. Frequency indices are normalized by the width of the signal sampling baseband.

Section 5.4 will compare discrete sinc interpolation with other methods and provide experimental evidence of its perfect performance and superiority.

5.3 Fast Algorithms of Discrete Sinc Interpolation and Their Applications

5.3.1 Signal sub-sampling with DFT or DCT spectral zero-padding

One of the basic image resampling tasks is image sub-sampling (zooming in), i.e., computing a set of intermediate samples from the given set of samples. From properties of signal DFT spectra of sparse signals, discussed in Appendix A2.9 (Eqs. (A2.47), (A2.48), (A2.50), and (A2.61)) it follows that discrete sinc interpolated signal sub-sampling can be achieved by zero-padding its DFT spectrum. Given the desired nomber N of the zoomed-in signal samples and the number N_0 of samples of the original signal, this algorithm is described by the following equation:

$$\tilde{a}_{\tilde{k}} = \mathrm{IFFT}_N\{\mathrm{DFT\_ZP}_{N/N_0}[\mathrm{FFT}_{N_0}(a_k)]\}, \tag{5.19}$$

where $\{a_k\}$, $k = 0, 1, \ldots, N_0 - 1$ are the initial signal samples, $\{\tilde{a}_{\tilde{k}}\}$ are zoomed-in signal samples, $\tilde{k} = 0, 1, \ldots N - 1$, $\mathrm{FFT}_{N_0}(\cdot)$ and $\mathrm{IFFT}_N(\cdot)$ are N_0-point direct and N-point inverse fast Fourier transform operators, respectively, and $\mathrm{DFT\_ZP}_{N/N_0}[\,\cdot\,]$ is a zero-padding operator. The zero-padding

Chapter 6
Discrete Sinc Interpolation in Other Applications and Implementations

6.1 Precise Numerical Differentiation and Integration of Sampled Signals

6.1.1 Perfect digital differentiator and integrator

Signal numerical differentiation and integration are operations that require measuring infinitesimal increments of signals and their arguments. Therefore, the numerical computation of signal derivatives and integrals assumes the building of "continuous" models of signals specified by their samples through explicit or implicit interpolation between available signal samples.

Because differentiation and integration are shift-invariant linear operations, methods of computing signal derivatives and integrals from their samples can be conveniently designed and compared in the Fourier transform domain. Let the Fourier transform spectrum of a continuous signal $a(x)$ be $\alpha(f)$:

$$a(x) = \int_{-\infty}^{\infty} \alpha(f) \exp(-i2\pi f x) df. \tag{6.1}$$

Then the Fourier spectrum of its derivative

$$\frac{d}{dx} a(x) = \int_{-\infty}^{\infty} [(-i2\pi f)\alpha(f)] \exp(-i2\pi f x) df \tag{6.2}$$

will be $(-i2\pi f)\alpha(f)$, and the Fourier spectrum of its integral

$$\bar{a}(x) = \int a(x) dx = \int_{-\infty}^{\infty} \left[\left(-\frac{1}{i2\pi f} \right) \alpha(f) \right] \exp(-i2\pi f x) df \tag{6.3}$$

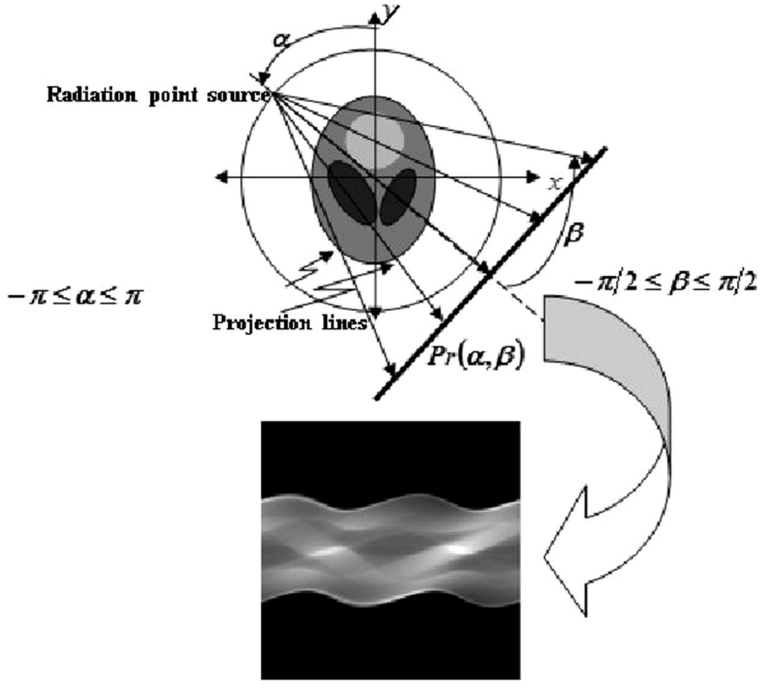

Figure 6.11 Geometry of image fan projections.

(for each position angle α of the point source) projections $Pr(\alpha, \beta)$ as a function of the ray angles β. A set of projections for $-\pi \le \alpha \le \pi$ is then used for image reconstruction.

In principle, inverting the RT in fan-beam projection geometry requires reconstruction algorithms that work in fan-beam projection geometry. There is however an alternative and attractive option of converting, by an appropriate resampling, the set of fan projections into a set of parallel projections and to enable in this way image reconstruction with algorithms for image reconstruction from parallel projections. For the resampling, one can use the above described algorithms for resampling by image sub-sampling using global or local discrete sinc interpolation. The latter can, if required, be combined with denoising, as discussed in Section 6.2. This process of converting one type of projection into another type is called *data rebinning*. Figure 6.12 illustrates this method of image reconstruction.

6.4 Exercises

differentiator_comparison_SPIE.m

Comparison of signal differentiation accuracy of two conventional differentiators with point spread functions

Chapter 9
Discrete Representation of the Convolution Integral

9.1 Discrete Convolution

In signal theory, the convolution integral

$$b(x) = \int_{-\infty}^{\infty} a(\xi)h(x-\xi)d\xi \tag{9.1}$$

is a mathematical model of shift-invariant filtering signal $a(x)$ by a linear filter with point spread function (PSF) $h(x)$. A discrete representation of the convolution intergral can be obtained by finding a relationship between samples

$$b_k = \int_{-\infty}^{\infty} b(x)PSF^{(s)}(k\Delta_x - x)dx \tag{9.2}$$

of the convolution result $b(x)$ with samples $\{a_n\}$ of the convolved signal $a(x)$. Insert Eq. (9.1) in Eq. (9.2) and replace the former signal $a(x)$ with its expression (Eq. (8.2)) through its samples $\{a_n\}$:

$$\begin{aligned} b_k &= \int_{-\infty}^{\infty}\left[\int_{-\infty}^{\infty} a(\xi)h(x-\xi)d\xi\right]PSF^{(s)}(k\Delta_x - x)dx \\ &= \int_{-\infty}^{\infty} PSF^{(s)}(k\Delta_x - x)dx\left\{\int_{-\infty}^{\infty}\left[\sum_n a_n PSF^{(r)}(\xi - n\Delta_x)\right]h(x-\xi)d\xi\right\} \\ &= \sum_{n=-\infty}^{\infty} a_n \int_{-\infty}^{\infty}\int_{-\infty}^{\infty} h(\xi - x + (k-n)\Delta_x)PSF^{(r)}(\xi)PSF^{(s)}(x)d\xi dx \\ &= \sum_{n=-\infty}^{\infty} a_n h_{k-n}, \end{aligned} \tag{9.3}$$

Appendix 2
Discrete Fourier Transforms and Their Properties

A2.1 Invertibility of Discrete Fourier Transforms and the Discrete Sinc Function

Consider the general scaled shifted DFT of a signal with samples $\{a_k\}$

$$\alpha_r = \frac{1}{\sqrt{\lceil \sigma N \rceil}} \sum_{n=0}^{N-1} a_n \exp\left(i2\pi \frac{\tilde{n}\tilde{r}}{\lceil \sigma N \rceil} \right);\ \tilde{n} = n + u;\ \tilde{r} = r + v \tag{A2.1}$$

and show that its inverse is the transform

$$a_k = \frac{1}{\sqrt{\lceil \sigma N \rceil}} \sum_{r=0}^{\lceil \sigma N \rceil - 1} \alpha_r \exp\left(-i2\pi \frac{\tilde{k}\tilde{r}}{\lceil \sigma N \rceil} \right);\ \tilde{k} = k + u;\ \tilde{r} = r + v. \tag{A2.2}$$

Insert the expression Eq. (A2.1) for $\{\alpha_r\}$ into Eq. (A2.2) to obtain

$$\begin{aligned}
a_k &= \frac{1}{\sqrt{\lceil \sigma \mathrm{N} \rceil}} \sum_{r=0}^{\lceil \sigma N \rceil - 1} \alpha_r \exp\left(-i2\pi \frac{\tilde{k}\tilde{r}}{\lceil \sigma N \rceil} \right) \\
&= \frac{1}{\lceil \sigma N \rceil} \sum_{r=0}^{\lceil \sigma N \rceil - 1} \left[\sum_{n=0}^{N-1} a_n \exp\left(i2\pi \frac{\tilde{n}\tilde{r}}{\lceil \sigma N \rceil} \right) \right] \exp\left(-i2\pi \frac{\tilde{k}\tilde{r}}{\lceil \sigma N \rceil} \right) \\
&= \frac{1}{\lceil \sigma N \rceil} \sum_{n=0}^{N-1} a_n \sum_{r=0}^{\lceil \sigma N \rceil - 1} \exp\left[i2\pi \frac{(n-k)}{\lceil \sigma N \rceil} (r + v) \right] \\
&= \frac{\exp\left[i2\pi \frac{(n-k)}{\lceil \sigma N \rceil} v \right]}{\lceil \sigma N \rceil} \sum_{n=0}^{N-1} a_n \frac{\exp[i2\pi(n-k)] - 1}{\exp\left(i2\pi \frac{n-k}{\lceil \sigma N \rceil} \right) - 1}
\end{aligned}$$